Supplementary Information for

"Astrocyte-derived TNF and glutamate critically modulate microglia activation by methamphetamine" by Canedo et al.

Contents within the present file

Guide for Other Supplementary materials (available as individual files):

Suppl. Table 1 – Genes enriched in microglia Meth vs Saline (Data Set).
Suppl. Table 2 – List of all genes identified in microglia Meth vs Saline (Data Set).
Suppl. Table 3 – GSEA data (Data Set).
Suppl. Video 1 – Primary astrocytes from WT mice expressing the glutamate release FRET biosensor (FLIPE) exposed to Meth 100µM (support Fig. 3B and Supp. Fig 4D).
Suppl. Video 2 - Primary astrocytes from TNF KO mice expressing the glutamate release FRET biosensor (FLIPE) exposed to Meth 100µM (support Fig. 3B and Supp. Fig 4D).

1. Supplementary methods

Bioinformatical Analysis of Microglial RNA sequencing

Data from the S5 XL run processed using the Ion Torrent platform specific pipeline software Torrent Suite v5.12 to generate sequence reads, trim adapter sequences, filter and remove poor signal reads, and split the reads according to the barcode. FASTQ and/or BAM files were generated using the Torrent Suit plugin FileExporter v5.12. Automated data analysis was done with Torrent Suite™ Software using the Ion AmpliSeq™ RNA plug-in v.5.12 and target region AmpliSeq_Mouse_Transcriptome_V1_Designed.

Raw data was loaded into the Transcriptome Analysis Console (4.0 Thermo Fisher Scientific, MA, USA) and first filtered based on ANOVA eBayes using Limma package, applied to fold changes ≤ -1.5 or ≥1.5 between experimental and control conditions. Significant changes had a *p* value <0.05 and a false discovery rate <0.2. Genes that were significantly downregulated or upregulated by Meth in microglia, following the described criteria, are listed in **Supp. Table 1.**

RNA-seq functional enrichment analysis using Gene Set Enrichment Analysis (GSEA) was performed by WEB-based Gene SeT AnaLysis Toolkit (WebGestalt) [81]. All detectable genes (**Supp. Table 2**) with their corresponding fold-change values were submitted to WebGestalt at http:// http://www.webgestalt.org. GSEA was performed using the open-access available platforms, Wikipathways, KEEG and REACTOME with default settings. Enrichment scores for gene sets were calculated using an FDR cutoff of 0.05 and hypergeometric overlap analysis **(Supp. Table 3)**. Genes retrieved from GSEA datasets were used for constructing a protein-protein interaction network. Such network was generated using Omics Visualizer [82] and String applications [83] in Cytoscape.

Cell viability assay

Cells were fixed with 4% PFA for 10 min and then stained with 1µg/ml Hoechst 33342 (Sigma-Aldrich) for 30 min at 37 °C. After wash, cells were observed using a DMI6000B inverted microscope (Leica Microsystems) with an HCX Plan Apo 63x/1.3 NA glycerol immersion objective. Images were acquired with 4x4 binning using a digital CMOS camera (ORCA-Flash4.0 V2, Hamamatsu Photonics). For quantification cells with condensed or fragmented nuclei were defined as dead cells.

Automated fluorescence imaging and quantification

Primary microglial cells were seeded on 96-well plate (CellCarrier, PerkinElmer, MA, USA) at 1 x 10^4 cells/well using an automated Multidrop dispenser (Thermo Scientific). Twenty-four hours after glutamate or ACM exposure, microglial cells were washed and fixed with 4% PFA

(w/v). Cells were then permeabilized with 0.25% (v/v) Triton X-100 for 10 min at room temperature and incubated with primary antibody (**Suppl. Table 5**) for 24h at 4ºC. After washes, secondary antibodies conjugated with Alexa Fluor 568 were incubated for 1h (RT). Antibodies were described in **Supp. Table 5**. Hoescht (0,5 µg/mL) and HCS CellMask (Invitrogen) were incubated for 30min (RT).

Images of microglial cultures were acquired in INCell Analyzer 2000 microscope (GE Healthcare, IL, USA) using a large chip CCD Camera (binning 2X2) and a Nikon 40x/0.95 NA Plan Fluor objective. Image analysis was performed using the CellProfiler (4.2.0) program. Briefly, the image analysis workflow consists in the segmentation of the nuclei, using the Hoechst channel followed by Otsu local thresholding. Afterward, microglial cells were segmented using the raw HCS CellMask image through a propagation algorithm based on the minimum cross entropy thresholding method applied to the HCS CellMask channel. The mean pixel intensity of the interest channels in each individual cell were extracted and plotted for evaluation.

2. Supplementary Figures and Legends

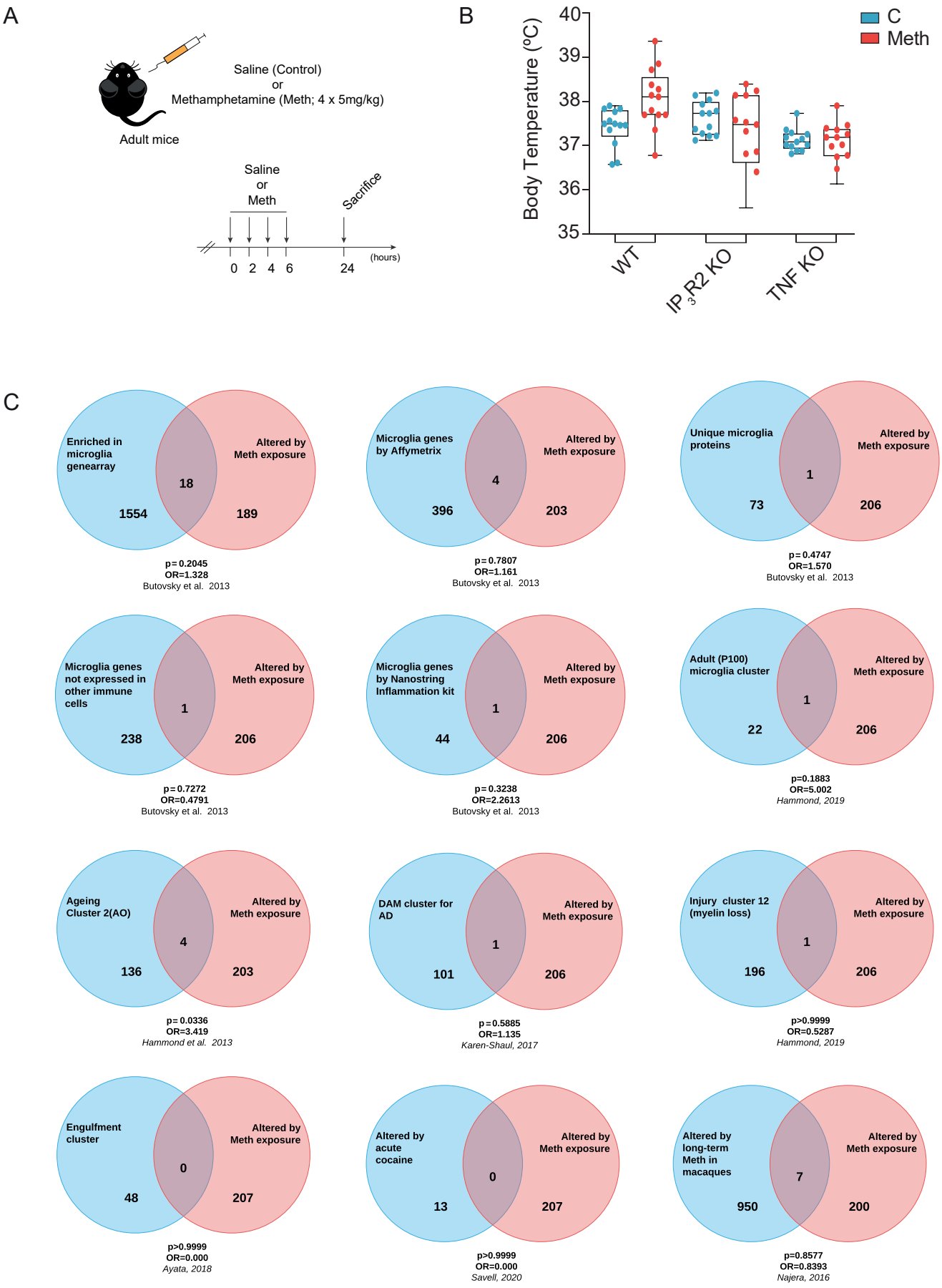
A
Saline (Control)
or
Methamphetamine (Meth; 4 x 5mg/kg)
Adult mice
Saline
or
Meth
Sacrifice
0 2 4 6
24
(hours)
B
C
Meth
Body Temperature (°C)
40
39
38
37
36
35
WT
IP3R2 KO
TNF KO
C
Enriched in microglia genearray
1554
18
Altered by Meth exposure
189
p = 0.2045
OR=1.328
Butovsky et al. 2013
Microglia genes by Affymetrix
396
4
Altered by Meth exposure
203
p = 0.7807
OR=1.161
Butovsky et al. 2013
Unique microglia proteins
73
1
Altered by Meth exposure
206
p = 0.4747
OR=1.570
Butovsky et al. 2013
Microglia genes not expressed in other immune cells
238
1
Altered by Meth exposure
206
p = 0.7272
OR=0.4791
Butovsky et al. 2013
Microglia genes by Nanostring Inflammation kit
44
1
Altered by Meth exposure
206
p = 0.3238
OR=2.2613
Butovsky et al. 2013
Adult (P100) microglia cluster
22
1
Altered by Meth exposure
206
p=0.1883
OR=5.002
Hammond, 2019
Ageing Cluster 2(AO)
136
4
Altered by Meth exposure
203
p = 0.0336
OR=3.419
Hammond et al. 2013
DAM cluster for AD
101
1
Altered by Meth exposure
206
p = 0.5885
OR=1.135
Karen-Shaul, 2017
Injury cluster 12 (myelin loss)
196
1
Altered by Meth exposure
206
p>0.9999
OR=0.5287
Hammond, 2019
Engulfment cluster
48
0
Altered by Meth exposure
207
p>0.9999
OR=0.000
Ayata, 2018
Altered by acute cocaine
13
0
Altered by Meth exposure
207
p>0.9999
OR=0.000
Savell, 2020
Altered by long-term Meth in macaques
950
7
Altered by Meth exposure
200
p=0.8577
OR=0.8393
Najera, 2016

Suppl. Fig. 1

Supplementary Figure 1.

A: Schematic representation of binge Meth administration.

B: WT, IP_3R2 KO, and TNF KO mice were administered saline (CT) or Meth. The whisker plots represent the median (line within the box), maximum (top whisker) and minimum (bottom whisker) values of mice's body temperature during the Meth administration protocol. Temperatures were evaluated at 13 time points, each point represents the mean temperature (n=3 animals *per* group) for one timepoint.

C: Venn's diagrams representing cluster analysis comparing the 207 Meth-altered genes cluster found in our RNA-seq analysis, with clusters previously reported for healthy[4,5], aging[6], disease-associated (DAM)[7], injured[6], drug exposed microglia[8,9], or with clusters previously associated to specific microglia functions[4]. Comparisons were conducted by contingency analysis, using the Fisher's exact test and the Baptista-Pike method to calculate the odds-ratio. Significance was set at $p<0.05$. A comprehensive list of the shared genes in each case is available in **Suppl. Table 7**.

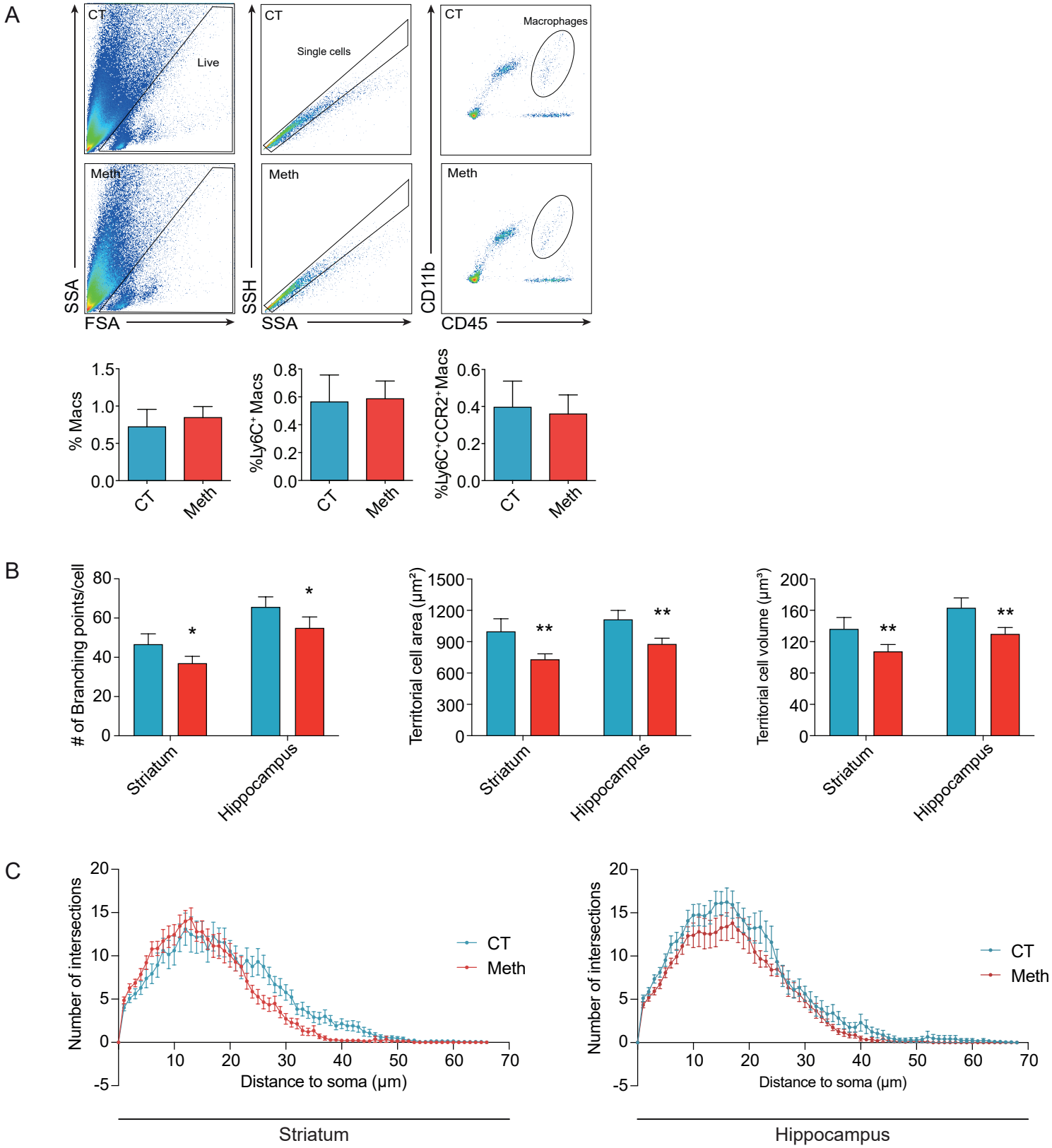
A
CT
Live
Meth
SSA
FSA
CT
Single cells
Meth
SSH
SSA
CT
Macrophages
Meth
CD11b
CD45
% Macs
%Ly6C⁺ Macs
%Ly6C⁺CCR2⁺Macs
CT
Meth
B
# of Branching points/cell
Territorial cell area (µm²)
Territorial cell volume (µm³)
Striatum
Hippocampus
C
Number of intersections
Distance to soma (µm)
CT
Meth
Striatum
Hippocampus

Suppl. Fig. 2

Supplementary Figure 2.

A: Flow cytometry analyses of macrophages ($CD11b^+$ $CD45^{high}$) isolated from the brains of mice injected with binge Meth or saline (CT) (n=5 animals *per* group). Graphs display with mean and SEM of the percentage of macrophages, the percentage of macrophages expressing activation markers such as $Ly6C^+$ and $Ly6C^+CCR2^+$.

B: Morphological analyses of microglia from striatal or hippocampal sections from mice administered with binge Meth or saline (CT). Graphs display (mean and SEM) of Imaris-based automated quantification for the number of branching points, territorial cell area and territorial cell volume (13-17 cells/group from n=3 mice *per* group). *p<0.05, **p<0.001 (unpaired t test). Two-way ANOVA (treatment x region) reveling also a significant effect for region (p<0.05) for branching points (p<0.001) and territorial volume (p<0.05), followed by the two-stage linear step-up procedure of Benjamini, Krieger and Yekutieli.

C: Sholl analysis of microglia from striatal or hippocampal sections from mice administered with binge Meth or saline (CT) (13-17 cells/group from n=3 mice *per* group). Two-way ANOVA revealing significant effects for treatment and distance to soma: striatum (p<0.001, p<0.0001), hippocampus (p<0.0001, p<0.0001), but no interaction between factors.

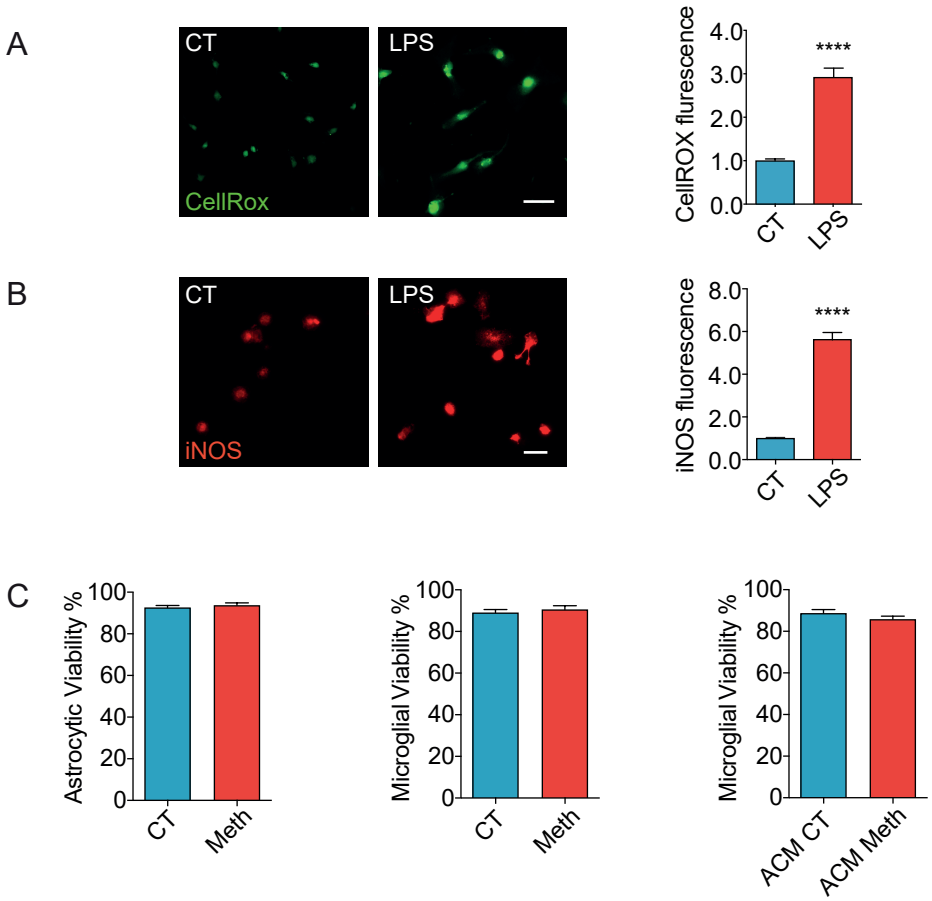
A
CT
LPS
CellRox
CellROX flurescence
4.0
3.0
2.0
1.0
0.0
****
CT
LPS
B
CT
LPS
iNOS
iNOS fluorescence
8.0
6.0
4.0
2.0
0.0
****
CT
LPS
C
Astrocytic Viability %
100
80
60
40
20
0
CT
Meth
Microglial Viability %
100
80
60
40
20
0
CT
Meth
Microglial Viability %
100
80
60
40
20
0
ACM CT
ACM Meth
D
Striatum
Hippocampus
TNF mRNA levels
20.0
15.0
10.0
5.0
0.0
**
CT
Meth
TNF mRNA levels
12.0
9.0
6.0
3.0
0.0
CT
Meth
IL-1β mRNA levels
6.0
5.0
4.0
3.0
2.0
1.0
0.0
CT
Meth
IL-1β mRNA levels
5.0
4.0
3.0
2.0
1.0
0.0
*
CT
Meth
IL-6 mRNA levels
3.0
2.0
1.0
0.0
CT
Meth
IL-6 mRNA levels
3.0
2.0
1.0
0.0
CT
Meth

Suppl. Fig. 3

Supplementary Figure 3.

A: Primary microglia cells incubated with the CellRox® green reagent and treated with 1µg/mL LPS for 24h (n=3 independent cultures). Graph (means and SEM) displays the CellRox® intensity normalized to the control values. ****p<0.0001 (unpaired t-test). Scale bar 10µm.
B: Fluorescence imaging of primary microglia immunolabeled for iNOS treated with 1µg/mL LPS for 24h (n=3 independent cultures). Graph (means and SEM) displays iNOS intensity normalized to the Control values. ****p<0.0001 (unpaired t test). Scale bar 10µm.
C: Viability of astrocytes were examined by Hoechst staining under 100µM Meth. Graphs represent (means and SEM) the percentage of astrocyte or microglia viability upon Meth exposure compared to control (CT) condition, and percentage of viability for microglia upon ACM Meth exposure compared to the control condition (ACM CT).
D: qRT-PCR for TNF, IL-1β and IL-6 from the striatum or hippocampus of WT mice administered with saline or Meth (n=5 mice *per* group). Graphs (means and SEM) display the mRNA levels of indicated transcripts. *p<0.05 and **p<0.01 (unpaired t-test).

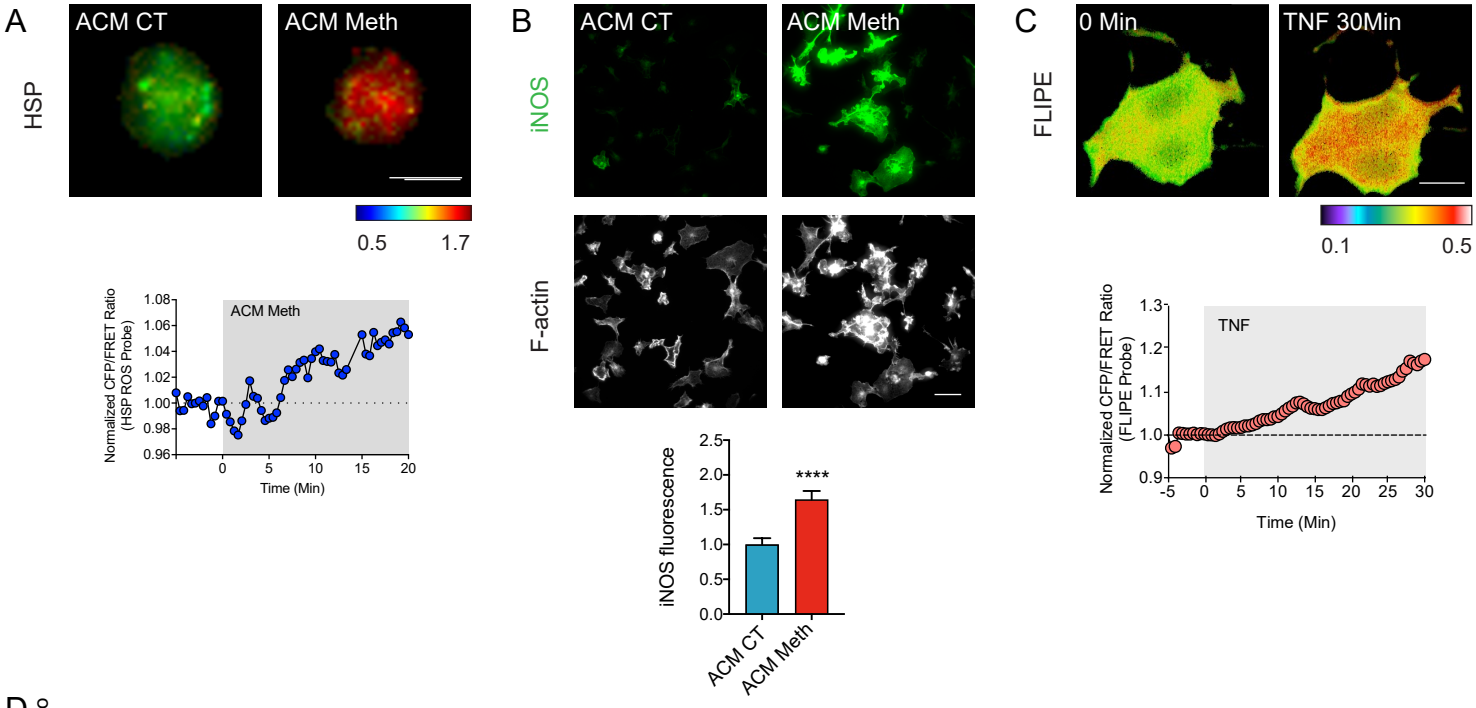
A
ACM CT
ACM Meth
HSP
0.5
1.7
Normalized CFP/FRET Ratio (HSP ROS Probe)
ACM Meth
Time (Min)
B
ACM CT
ACM Meth
iNOS
F-actin
iNOS fluorescence
****
ACM CT
ACM Meth
C
0 Min
TNF 30Min
FLIPE
0.1
0.5
Normalized CFP/FRET Ratio (FLIPE Probe)
TNF
Time (Min)

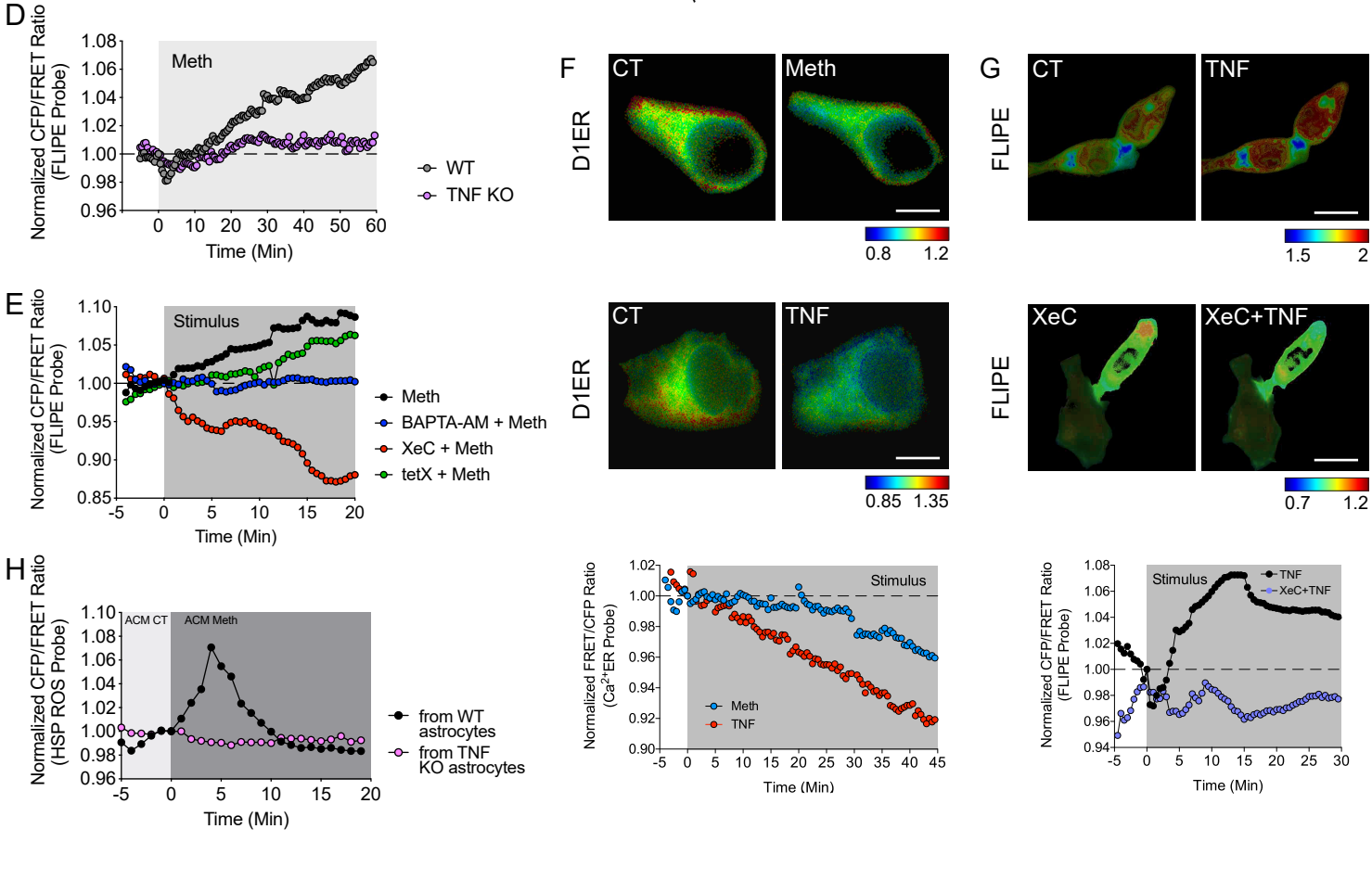
D
Normalized CFP/FRET Ratio (FLIPE Probe)
Meth
WT
TNF KO
Time (Min)
F
CT
Meth
D1ER
0.8
1.2
G
CT
TNF
FLIPE
1.5
2
E
Normalized CFP/FRET Ratio (FLIPE Probe)
Stimulus
Meth
BAPTA-AM + Meth
XeC + Meth
tetX + Meth
Time (Min)
CT
TNF
D1ER
0.85
1.35
XeC
XeC+TNF
FLIPE
0.7
1.2
H
Normalized CFP/FRET Ratio (HSP ROS Probe)
ACM CT
ACM Meth
from WT astrocytes
from TNF KO astrocytes
Time (Min)
Normalized FRET/CFP Ratio (Ca2+ER Probe)
Stimulus
Meth
TNF
Time (Min)
Normalized CFP/FRET Ratio (FLIPE Probe)
Stimulus
TNF
XeC+TNF
Time (Min)

Suppl. Fig. 4

Supplementary Figure 4.

A: Primary microglia expressing the ROS FRET biosensor (HSP) were incubated with ACM CT (left panel) and then exposed to ACM Meth (right panel). Time-lapses of CFP/FRET ratio changes for the HSP biosensor (normalized at 0 min) are shown according to the scale (n=4 cells pooled across 2 independent experiments). Scale bars 10µm.

B: Fluorescence imaging of primary microglia immunolabeled for iNOS (green) and F-actin (grey; labeled with Alexa Fluor 647 Phalloidin obtained from Thermo Scientific) and treated with ACM CT or ACM Meth for 24h (n=3 independent experiments). Graph (means and SEM) displays iNOS intensity normalized to the ACM CT. ****p<0.0001 (unpaired t-test). Scale bar 10µm.

C: Primary astrocytes expressing the glutamate release FRET biosensor (FLIPE) were exposed to TNF (50nM). Time-lapses of CFP/FRET ratio changes for the FLIPE biosensor (normalized at 0 min) are shown according to the scale (n=6 cells pooled across 2 independent experiments). Scale bars 10µm.

D: Time-lapses of CFP/FRET ratio changes for the FLIPE biosensor (normalized at 0 min) for the glutamate release illustrated in Fig. 3B shown according to the scale (n=3-8 cells pooled across 2-3 independent experiments).

E: Time-lapses of CFP/FRET ratio changes for the FLIPE biosensor (normalized at 0 min) for the glutamate release experiments illustrated in Fig. 3C shown according to the scale (n=5-7 cells pooled across 3 independent experiments)**.**

F: Primary astrocytes expressing the endoplasmic reticulum calcium release FRET biosensor (D1ER) were exposed to Meth (100µM) (upper panels; blue circles) or TNF (50nM) (bottom panels; red circles). Time-lapses of CFP/FRET ratio changes for the D1ER biosensor (normalized at 0 min) are shown according to the scale (n=3-4 cells pooled across 2-3 independent experiments). Scale bars, 10µm.

G: Primary astrocytes expressing the glutamate release FRET biosensor (FLIPE) were exposed to TNF (50nM) (upper panels; black circles) or XestospongiC (500nM) + TNF (50nM) (bottom panels; lilac circles). Time-lapses of CFP/FRET ratio changes for the FLIPE biosensor (normalized at 0 min) are shown according to the scale (n=4 cells pooled across 2 independent experiments). Scale bars, 20µm.

I: Time-lapses of CFP/FRET ratio changes for the ROS FRET biosensor (HSP) normalized at 0 min, for the glutamate release illustrated in Fig. 3G shown according to the scale (n=4 cells pooled across 2 independent experiments).

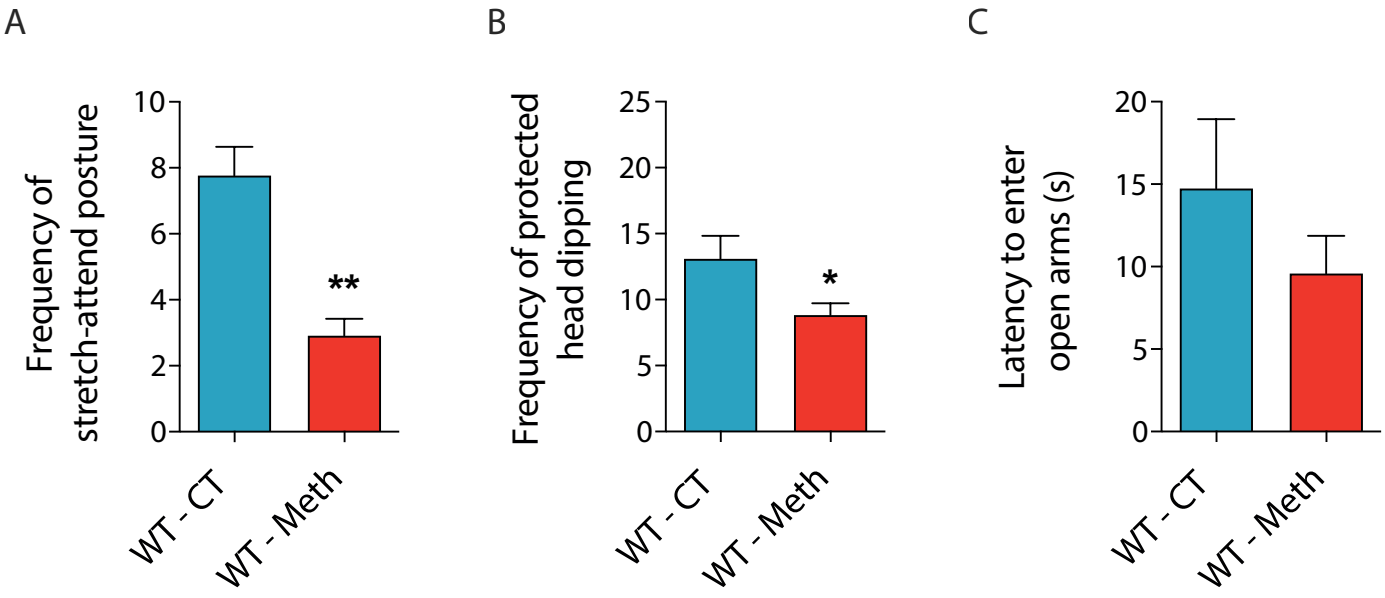
A
Frequency of stretch-attend posture
10
8
6
4
2
0
**
WT - CT
WT - Meth
B
Frequency of protected head dipping
25
20
15
10
5
0
*
WT - CT
WT - Meth
C
Latency to enter open arms (s)
20
15
10
5
0
WT - CT
WT - Meth

Suppl. Fig. 5

Supplementary Figure 5.

A: WT animals were evaluated in the EPM 24 hours after being administered with saline (CT) or binge Meth (n=11-13 animals *per* group). CT and Meth-treated mice displayed significant differences in the frequency of stretch-attend postures (SAP). The graph displays the mean and SEM. **p<0.01 (unpaired t test).

B: WT animals were evaluated in the EPM 24 hours after being administered with saline (CT) or binge Meth (n=11-13 animals per group). CT and Meth-treated mice displayed significant differences in the frequency of protected head dipping. The graph displays the mean and SEM. *p<0.05 (unpaired t test).

C: WT animals were evaluated in the EPM 24 hours after being administered with saline (CT) or binge Meth (n=11-13 animals per group). CT and Meth-treated mice displayed no differences regarding the latency to enter in open arms. The graph displays the mean and SEM.

3. Supplementary tables

Supplementary Table 4. Antibodies used for immunohistochemistry

Antibody	Dilution	Company
CD68	1:500	Abcam (CAM, UK)
GFAP	1:500	Abcam (CAM, UK)
Iba-1	1:500	Wako (CA, USA)
TNF	1:500	Peprotech (LND, UK)
Anti-mouse Alexa 488	1:1000	Life Technologies (CA, USA)
Anti-rabbit Alexa 568	1:1000	Life Technologies (CA, USA)

Supplementary Table 5. Antibodies used for immunocytochemistry

Antibody	Dilution	Company
Arginase 1	1:100	Santa Cruz Biotechnology (TX, USA)
CD11b	1:200	Abcam (CAM, UK)
CD68	1:200	Bio-Rad (CA, USA)
iNOS	1:200	Santa Cruz Biotechnology (TX, USA)
Anti-mouse Alexa 488	1:1000	Life Technologies (CA, USA)
Anti-rabbit Alexa 568	1:1000	Life Technologies (CA, USA)

Supplementary Table 6. Primer sequences used in qRT-PCR

Primer	Forward (5' - 3')	Reverse (5' - 3')
IL-10 (Rat)	ATCCGGGGTGACAATAACTG	TGTCCAGCTGGTCCTTCTTT
IL-1β (Ms)	GCCCATCCTCTGTGACTCAT	AGGCCACAGGTATTTTGTCG
IL-1β (Rat)	TAAGCCAACAAGTGGTATTC	AGGTATAGATTCTTCCCCTTG
IL-6 (Ms)	CACAAGTCCGGAGAGGAGAC	CAGAATTGCCATTGCACAAC
IL-6 (Rat)	ACTCATCTTGAAAGCACTTG	GTCCACAAACTGATATGCTTAG
iNOS (Rat)	AGCCGTAACAAAGGAAATAG	ATGCTGGAACATTTCTGATG
S18 (Ms)	GCCATTAAGGGCGTGGGG	GTGATCACTCGCTCCACCTC
TGF-β (Rat)	TGAGTGGCTGTCTTTTGACG	GTTTGGGACTGATCCCATTG
TNF (Ms)	GCCACCACGCTCTTCCTGTCT	TGAGGGTCTGGGCCATAGAAC
TNF (Rat)	CTCACACTCAGATCATCTTC	GAGAACCTGGGAGTAGATAAG
Ywhaz (Rat)	GATGAAGCCATTGCTGAACTTG	GTCTCCTTGGGTATCCGATGTC

Supplementary Table 7: Genes overlapping between published gene sets and enriched genes in microglia Meth vs Saline

Cluster analysed	Referece	Total number of genes compared	Intersection	Fisher's exact test (p value)	Odds ratio	Intersection genes
Genes enriched in microglia based on Genearray analysis.	Butovsky, 2013 [85]	1572	18	0.2045	1.328	Srl; Ears2; Zfp846; Urgcp; Gpr146; Pstk; Slc1a4; Tspan31; St6gal1; Pam; Ccrl2; Smo; Mras; Mtap; E2f5; Slc7a6; Procr; Vipr1
Enriched microglia and monocyte proteins identified by TMT-based quantitative proteomic analysis	Butovsky, 2013 [85]	455	4	0.8	1.017	Mtap; Rxrg; Slc4a2; Nop56
Enriched monocyte proteins identified by TMT-based quantitative proteomic analysis	Butovsky, 2013 [85]	926	8	0.9999	0.999	Hmha1; Crot; Iars2; Nadk; Srp68; Ranbp1; Fxyd5; Lgals1
Unique microglial proteins detected by TMT-based Mass spec	Butovsky, 2013 [85]	74	1	0.4747	1.57	Slc4a2
Microglial proteins detected by both TMT-based Mass spec and Gene Array	Butovsky, 2013 [85]	64	1	0.4269	1.819	Mtap
Microglial genes identified by Affymetrix genearray	Butovsky, 2013 [85]	400	4	0.7807	1.161	Tlr6; Agmo; Mras; Slc4a2;
Microglial genes highly expressed and/or affected in different neurinflammatory conditions detected by Nanostring Inflammation kit	Butovsky, 2013 [85]	46	1	0.3238	2.613	Tlr6
Microglia not expressed in other immune cells	Butovsky, 2013 [85]	239	1	0.7272	0.4791	Tlr6
Enriched in both microglia and organ macrophage	Butovsky, 2013 [85]	81	0	0.9999	0	
Adult cluster 1a (P100)	Hammond, 2019 [86]	23	1	0.1883	5.002	Lpl
Adult cluster 1b (P100)	Hammond, 2019 [86]	12	0	0.9999	0	
Aging Cluster 2(AO) (P540)	Hammond, 2019 [86]	136	4	0.0336	3.419	Lpl; Nfkbia; Fxyd5; Hmha1
Aging Cluster 3(AO) (P540)	Hammond, 2019 [86]	37	0	0.9999	0	
Aging Cluster MO (P540)	Hammond, 2019 [86]	288	3	0.741	1.21	Cd36; Fxyd5; Lgals1
Injury cluster 1 (saline injected myelin)	Hammond, 2019 [86]	201	1	0.9999	0.571	Lpl
Injury cluster 2 (LPC injected muelin)	Hammond, 2019 [86]	197	1	0.9999	0.5827	Lpl
DAM microglia (AD)	Karen-Shaul, 2017 [87]	102	1	0.5885	1.135	Lpl
Microglia enriched genes	Ayata, 2018 [84]	885	6	0.7098	0.7934	Tlr6; Cdr1; Hmha1; Neurl3;CD36; Lpl
Top 250 equally expressed in striatum and cerebellum	Ayata, 2018 [84]	250	4	0.1716	1.881	St6gal1; Papd4; Gpbp1l1; Nadk
Enriched in cerebellum microglia	Ayata, 2018 [84]	297	5	0.116	1.987	Zcchc3; Ubox5; Traf3ip1; Ccnd3; Fxyd5
Enriched in striatum microglia	Ayata, 2018 [84]	733	8	0.4202	1.276	Rin2; Srl; 9130023H24Rik; Hmha1; Neurl3; Ccrl2; Agmo; Mtap
Top 50 genes im microglia	Ayata, 2018 [84]	50	0	0.9999	0	
Engulfment Cluster	Ayata, 2018 [84]	48	0	0.9999	0	
Catabolism Cluster	Ayata, 2018 [84]	45	1	0.3238	2.613	Ubox5
Transcription cluster	Ayata, 2018 [84]	47	1	0.3355	2.499	Zcchc3
Cromatin modification cluster	Ayata, 2018 [84]	13	0	0.9999	0	
Altered genes in microglia after acute cocaine	Savell, 2020 [89]	13	0	0.9999	0	
Long term (23 w) Meth altered gens in macaques microglia	Najera, 2016 [88]	957	7	0.8577	0.8393	Pde6d; Prss16; Srm; Shmt1; Plekhg4; Lgals1; Mcm5
HIV altered gens in macaques microglia	Najera, 2016 (88]	1932	0	0.9999	0	

4. Supplementary references

81 Liao Y, Wang J, Jaehnig EJ, Shi Z, Zhang B. WebGestalt 2019: gene set analysis toolkit with revamped UIs and APIs. Nucleic Acids Research. 2019;47(W1):W199-W205.

82 Legeay M, Doncheva NT, Morris JH, Jensen LJ. Visualize omics data on networks with Omics Visualizer, a Cytoscape App. F1000Res. 2020;9:157.

83 Doncheva NT, Morris JH, Gorodkin J, Jensen LJ. Cytoscape StringApp: Network Analysis and Visualization of Proteomics Data. J Proteome Res. 2019;18(2):623-32.

84 Ayata P, Badimon A, Strasburger HJ, Duff MK, Montgomery SE, Loh Y-HE, et al. Epigenetic regulation of brain region-specific microglia clearance activity. Nat Neurosci. 2018;21(8):1049-60.

85 Butovsky O, Jedrychowski MP, Moore CS, Cialic R, Lanser AJ, Gabriely G, et al. Identification of a unique TGF-β–dependent molecular and functional signature in microglia. Nat Neurosci. 2014;17(1):131-43.

86 Hammond TR, Dufort C, Dissing-Olesen L, Giera S, Young A, Wysoker A, et al. Single-Cell RNA Sequencing of Microglia throughout the Mouse Lifespan and in the Injured Brain Reveals Complex Cell-State Changes. Immunity. 2019;50(1):253-71.e6.

87 Keren-Shaul H, Spinrad A, Weiner A, Matcovitch-Natan O, Dvir-Szternfeld R, Ulland TK, et al. A Unique Microglia Type Associated with Restricting Development of Alzheimer's Disease. Cell. 2017;169(7):1276-90.e17.

88 Najera JA, Bustamante EA, Bortell N, Morsey B, Fox HS, Ravasi T, et al. Methamphetamine abuse affects gene expression in brain-derived microglia of SIV-infected macaques to enhance inflammation and promote virus targets. BMC Immunol. 2016;17(1):7-7.

89 Savell KE, Tuscher JJ, Zipperly ME, Duke CG, Phillips RA, Bauman AJ, et al. A dopamine-induced gene expression signature regulates neuronal function and cocaine response. Sci Adv 2020;6(26):eaba4221.